Struct Chem (2013) 24:1241–1251
DOI 10.1007/s11224-012-0151-7

Synthesis, molecular structure, NMR spectroscopic and computational analysis of a selective adenosine A_{2A} antagonist, ZM 241385

Manuela Jörg · Mark Agostino · Elizabeth Yuriev · Frankie S. Mak · Neil D. Miller · Jonathan M. White · Peter J. Scammells · Ben Capuano

Received: 30 August 2012 / Accepted: 8 October 2012 / Published online: 27 October 2012

Abstract Herein, we describe the synthesis of the adenosine A_{2A} antagonist ZM 241385 (**9**) starting from commercially available 2-furanhydrazide (**1**) and including a comprehensive structural characterization of all the intermediates and the final product. In addition, extensive NMR analysis, including temperature and concentration-dependent experiments, are reported as well as the first single-crystal structure of the compound ZM 241385 (**9**) as the trihydrate. Furthermore, an extensive structural comparison of the single-crystal structure with the published protein bound X-ray structures is reported.

Keywords ZM 241385 · A_{2A} antagonist · Synthesis · Spectroscopic analysis · Crystal structure

Electronic supplementary material The online version of this article (doi:10.1007/s11224-012-0151-7) contains supplementary material, which is available to authorized users.

M. Jörg · M. Agostino · E. Yuriev · P. J. Scammells · B. Capuano (✉)
Medicinal Chemistry, Monash Institute of Pharmaceutical Sciences, 381 Royal Parade, Parkville, VIC 3052, Australia
e-mail: ben.capuano@monash.edu

M. Agostino
Western Australian Biomedical Research Institute, Curtin Health Innovation Research Institute, School of Biomedical Sciences, Curtin University, GPO Box U1987, Perth, WA 6845, Australia

F. S. Mak · N. D. Miller
GlaxoSmithKline, GSK R&D China, Singapore Research Centre, 11 Biopolis Way, Helios Bldg #03-01/02, Singapore 138667, Singapore

J. M. White
Bio21 Molecular Science & Biotechnology Institute, The University of Melbourne, 30 Flemington Road, Parkville, VIC 3010, Australia

Introduction

The recent interest in the adenosine A_{2A} receptor as a therapeutic target has significantly increased following studies that revealed the co-administration of an adenosine A_{2A} antagonist with a dopamine D_2 agonist showed promising clinical efficacy in the treatment of dyskinesias associated with Parkinson's disease therapy [1–3]. ZM 241385 (**9**) is a potent and selective adenosine A_{2A} antagonist [4] and the first ligand for which X-ray structures in complex with the adenosine A_{2A} receptor have been solved [5, 6]. The molecule exhibits a distinctive 2-(furan-2-yl)-[1,2,4]triazolo[1,5-*a*][1,3,5]triazin-7-amine scaffold and has been extensively used as a lead compound for various structure–activity relationship studies [2, 7, 8]. Nevertheless, limited experimental data and no comprehensive structural characterization (including X-ray crystal structure) or analysis of the NMR spectral characteristics has been published to date. Furthermore, the comparison of the two published protein bound X-ray structures showed some interesting differences which will be discussed later.

Synthesis

ZM 241385 (**9**) was synthesized according to the pathway illustrated in Scheme 1. The original patent synthesis of ZM 241385 [4] commenced with the precursor compounds aminoguanidine nitrate and 2-furonitrile. Our modified synthesis, although comparable with literature, commenced with commercially available 2-furanhydrazide (**1**) and incorporates relatively inexpensive reagents.

A mixture of furan-2-carbohydrazide (**1**), *S*-methylisothiourea (**2**), and sodium hydroxide in water was stirred at room temperature for 14 h and following work-up gave the

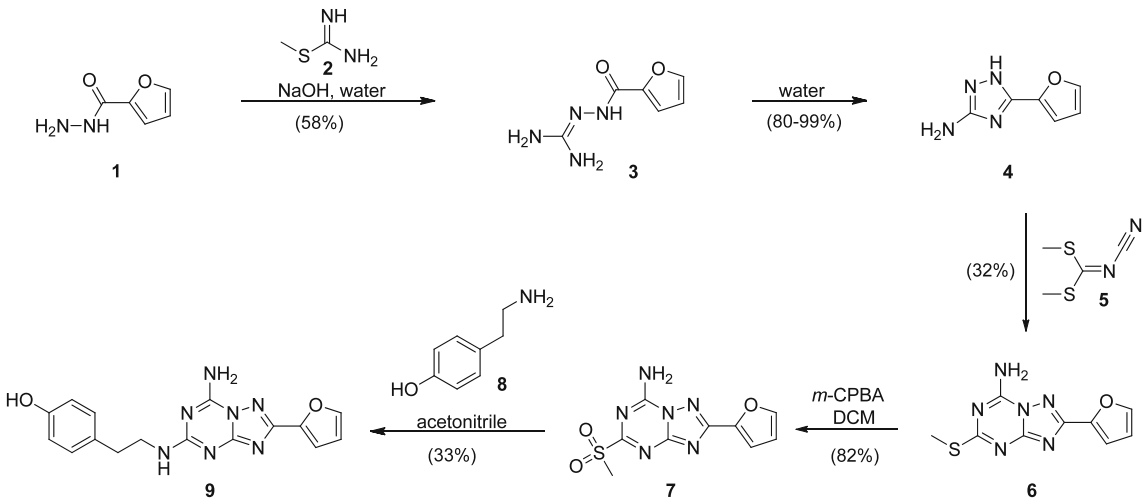

Scheme 1 Chemical synthesis of ZM 241385 (**9**)

furanoyl hydrazinecarboximidamide intermediate **3** in a moderate yield of 58 %. The yield obtained was consistent with that observed in the literature (52 % yield) [9]. The following step was accomplished by employing one of two methods published by Dolzhenko et al. [10], depending on reaction scale. On a scale up to 1 g, intermediate **3** was suspended in water and the reaction was performed in the microwave at 140 °C for 1 h before the solvent was removed under vacuum. The yield for this method was virtually quantitative (99 %). On a larger scale, the reaction of the aqueous suspension was performed using conventional heating at 100 °C for 29 h. The reaction volume was reduced and the precipitate filtered. Yields up to 80 % were achieved via the second method. 5-(Furan-2-yl)-1*H*-1,2,4-triazol-3-amine (**4**) was reacted with *N*-cyanodithioiminocarbonate (**5**) to afford **6** in 32 % yield after column chromatography [4, 11]. The sulfide intermediate **6** was subsequently oxidized with *m*-chloroperoxybenzoic acid at room temperature to afford the sulfone **7** in excellent yield (82 %) [4, 11]. Nucleophilic displacement of the methylsulfonyl group with tyramine (**8**) [4] furnished the target triazolotriazine (**9**, ZM 241385) in a 33 % yield with purity greater than 97 % as determined by analytical HPLC.

NMR analysis

Intermediates **6** and **7**, as well as the final compound ZM 241385 (**9**), showed very interesting and somewhat unexpected features in their respective NMR spectra. In this section, a number of NMR experiments are presented and the respective findings and interpretations are summarized and evaluated. Initially, we expected a broad singlet for the hydrogens of the NH_2 group for compounds **6** and **7** in the ^{1}H NMR, however, two broad singlets in a 1:1 ratio were actually observed (Figs. 1, 2). Caulkett et al. [11] observed the same phenomenon and demonstrated that the splitting was temperature-dependent; at 373 K the doublet coalesced to one singlet. In the case of compound **6**, we performed dilution experiments that showed the signal shape of the primary amine to be dependent on the concentration of the sample. Figure 1 shows two broad singlets (8.7–9.2 ppm) with a sample concentration of 7 mg/mL, one broad singlet at 1 mg/mL and again two broad singlets at 0.1 mg/mL. Dilution experiments (Fig. 2) were also performed with molecule **7**, but the signals never coalesced. Interestingly, when the compound [1,2,4]triazolo[1,5-*a*][1,3,5]triazin-7-amine (**10**) (Fig. 3) was analyzed under the same conditions, it did not exhibit any doubling up of the amino signal at any concentration.

The NMR spectra of ZM 241385 (**9**) not only exhibited splitting of the proton signals in the ^{1}H NMR spectrum, but also splitting of the carbon signals in the ^{13}C NMR spectrum. The NH_2 and NH groups of ZM 241385 (**9**) in the ^{1}H NMR spectrum in d_6-DMSO each displayed two signals in a ratio of 1:6 and 1:2, respectively. Figure 4 shows that the amino signals coalesced at 353 K into one broad singlet and one broad triplet for the NH_2 and NH groups, respectively. The splitting patterns of the CH_2 signals of the tyramine moiety in the proton spectrum also exhibit greater resolution at 353 K compared to 298 K.

Figure 5 shows the amino group resonances in the ^{1}H NMR spectra at different temperatures. A closer look revealed that the ratio of the two signals did not change, but rather the two signals moved closer together until they finally coalesced. At 303 K (red, spectrum 1), the two signals are clearly observed for each of the two amino groups (NH_2 and NH). By heating the sample in 10 K increments, the signals slowly moved closer together until they completely coalesced at 343 K, (dark blue, spectrum 5).

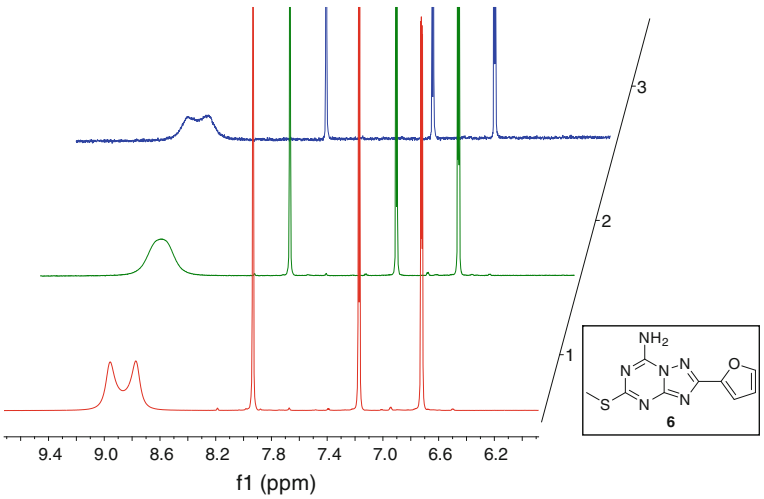

Fig. 1 Section of the ^{1}H NMR spectrum of compound **6,** which shows the NH_2 signals and the three furanyl protons at a sample concentration of 7 mg/mL (*red*, spectrum 1), 1 mg/mL (*green*, spectrum 2), and 0.1 mg/mL (*blue*, spectrum 3) (Color figure online)

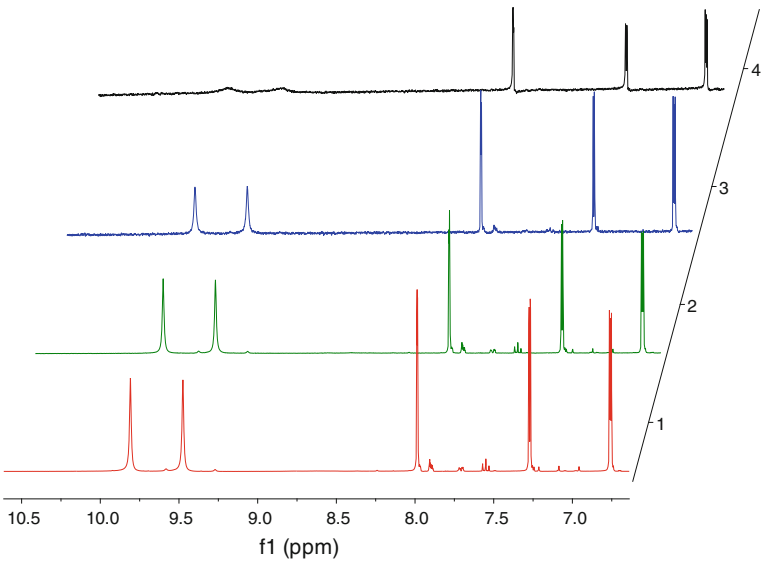

Fig. 2 Section of the ^{1}H NMR spectrum of compound **7** which shows the NH_2 signals and the three furanyl protons at a sample concentration of 7 mg/mL (*red*, spectrum 1), 1 mg/mL (*green*, spectrum 2), 0.1 mg/mL (*blue*, spectrum 3), and 0.01 mg/mL (*black*, spectrum 4) (Color figure online)

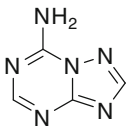

10

Fig. 3 Chemical structure of [1,2,4]triazolo[1,5-*a*][1,3,5]triazin-7-amine (**10**)

Unlike compounds **6** and **7**, for which no spectral anomalies were observed in their respective ^{13}C NMR spectra, the title compound, ZM 241385 (**9**), showed doubling up of most carbon signals. This effect was observed in both d_4-methanol and in d_6-DMSO. The doubled up carbon signals also exhibited a temperature-dependence, whereby they coalesced at 353 K (Fig. 6, blue spectrum).

Interestingly, the 2-(furan-2-yl)-5-phenethoxy-[1,2,4]triazolo[1,5-*a*][1,3,5]triazin-7-amine (**11**), which contains a phenethoxy moiety instead of the tyramine moiety, also exhibited doubling up of the amino group signal at position 7 in a 1:1 ratio, however, no anomalies were observed in the ^{13}C NMR spectrum (Fig. 7).

The splitting of the amino signal was not observed for compound **10**, therefore intramolecular interactions such as hydrogen bonding are unlikely to explain this phenomenon for intermediates **6** and **7**. Tautomerism was excluded due to the observations that (i) no additional carbon signals were observed, (ii) no additional cross peaks were present in the ^{15}N-^{13}C HQMC, and (iii) that it would be very unlikely to observe an exact 1:1 ratio of the amino signals for both compounds **6** and **7**. The fact that the signals in molecules **6** and **7** appear in exactly a 1:1 ratio, in addition to the observed temperature and concentration dependency, indicates that intermolecular interactions, such are dimer formation, are likely to be responsible for the observed doubling up of the amino group resonances.

In the case of the literature compound ZM 241385 (**9**), the spectral phenomena are more complex and we propose that this is due to the two effects occurring simultaneously, namely, intermolecular interactions, such as dimer formation,

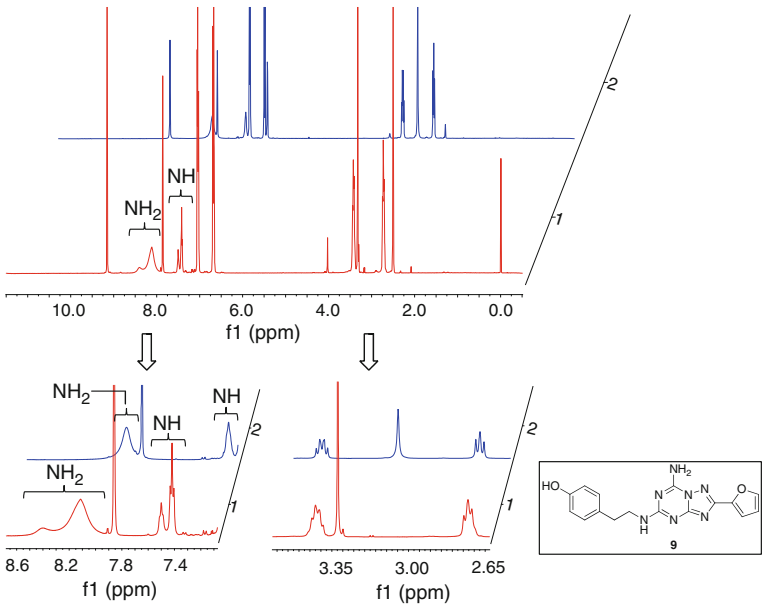

Fig. 4 ^{1}H NMR spectrum of ZM 241385 (**9**) at 298 K (*red*, spectrum 1) and 353 K (*blue*, spectrum 2) (*upper*). The *lower left* spectrum shows a zoomed section of the amino protons, that each show two signals at 298 K and one signal at 353 K. The *lower right* spectrum shows the CH_2 signals of the tyramine moiety at 298 and 353 K (Color figure online)

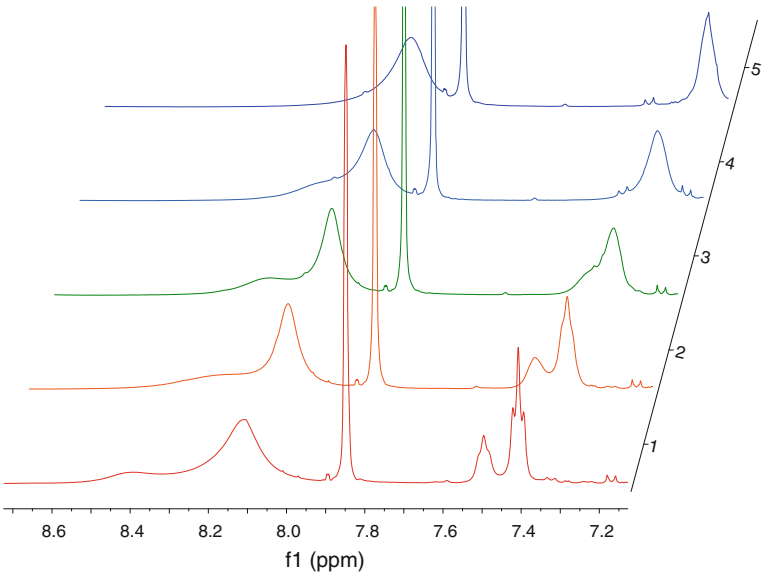

Fig. 5 ^{1}H NMR section of ZM 241385 (**9**) showing the amino protons at different temperatures (*red* = 303 K, spectrum 1; *orange* = 313 K, spectrum 2; *green* = 323 K, spectrum 3; *light blue* = 333 K, spectrum 4; *dark blue* = 343 K, spectrum 5). At 7.85 ppm is a singlet from an aromatic proton (Color figure online)

in conjunction with hindered rotation at the secondary amino group of the tyramine moiety. A comparison between molecules **9** and **11** shows that removing the secondary amine on the ligand in position 2 affects the ratio of the signals, but not the doubling up effect. This indicates that intermolecular interactions still occur but the second underlining effect has been eliminated. Some publications have examined similar effects caused either by nitrogen inversion or hindered rotation [12–14]. In the case of ZM 241385 (**9**), nitrogen inversion seems to be very unlikely due to the fact that the X-ray crystal structure of the molecule exhibits primarily sp^2 character for the amino group of the tyramine moiety (vide infra).

X-ray structure of ZM 241385

Crystals of the title compound **9** were grown by a two layer system of methanol and petroleum spirits. The crystals were used to generate an X-ray structure for ZM 241385 (**9**) that not only proved that the correct molecule was synthesized, but also gave interesting insight into the crystal packing. Compound **9** crystallizes with two independent molecules and six water molecules in the asymmetric unit as displayed in Fig. 8. The two molecules form a head-to-tail arrangement stabilized by hydrogen bonds (Fig. 9) between the hydroxyl groups (O1-H and O1′-H) on each molecule and the triazine nitrogens

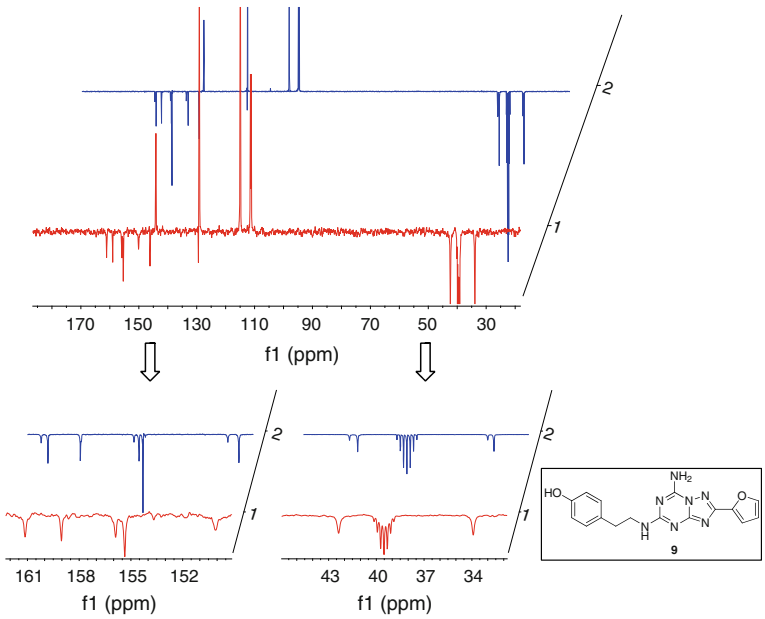

Fig. 6 ^{13}C NMR spectra of ZM 241385 (**9**) at 298 K (*blue*, spectrum 2) and 353 K (*red*, spectrum 1) (*upper*). The lower left spectrum shows a zoomed section of some of the quaternary carbons at 298 and 353 K. The *lower right* spectrum shows the CH_2 signals of the tyramine moiety that each show two signals at 298 K and a single resonance at 353 K (Color figure online)

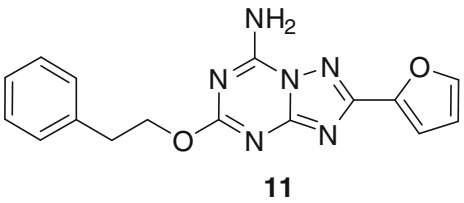

11

Fig. 7 Structure of 2-(furan-2-yl)-5-phenethoxy-[1,2,4]triazolo[1,5-*a*][1,3,5]triazin-7-amine (**11**)

(N6′ and N6) (see Table 1 for a complete list of hydrogen bond contacts in the crystal). The six water molecules form a cluster that helps to further stabilize the π-stacked layers of the ligand (Figs. 8, 10).

The crystal structure of ZM 241385 (**9**) revealed slight puckering of the triazine portion of the heterocycle (Table 2). Ideally, the torsions within the triazine should all be 0°, reflecting the aromaticity of the structure. However, one of the crystallographically determined structures revealed differences of up to 5° from the ideal predicted geometry.

Comparison of ZM 241385 crystal structures

The science of producing X-ray structures of receptors in complex with specific ligands has significantly improved the understanding of structure–function relationships and progressed the structure-based drug design to a new dimension. Nevertheless, obtaining ligand-bound X-ray structures in complex with G protein-coupled receptors, including the adenosine A_{2A} receptor, is still a challenging

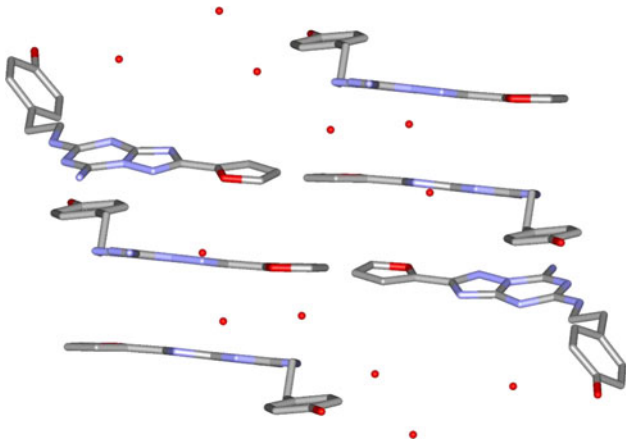

Fig. 8 Crystal packing of six ZM 241385 (**9**) molecules including water molecules (*red dots*) (Color figure online)

task due to problems such as low thermostability and low receptor expression levels [15]. In 2008, Jaakola et al. [5] published the first X-ray crystal structure (PDB 3EML) of the A_{2A} receptor in complex with the A_{2A} antagonist ZM 241385 (**9**), which revealed a unique ligand binding pocket (Fig. 11b). This X-ray structure was generated using a T4 lysozyme (T4L) fusion strategy. More recently, Doré et al. [6] published a second receptor bound X-ray structure (PDB 3PWH) of ZM 241385 (**9**) using a thermostabilized adenosine A_{2A} receptor (Fig. 11c). The two X-ray structures show subtle differences in their respective ligand interactions with the receptor, namely (i) the ligand is placed slightly deeper into the binding site in 3EML compared to 3PWH, and (ii) the conformation of tyrosine residues (Tyr9 and Tyr271 in the PDB sequences) near the phenol moiety of

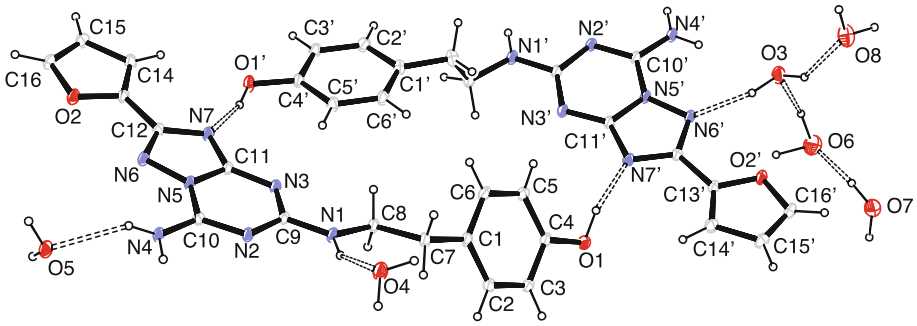

Fig. 9 Thermal ellipsoid plot for compound **9**. Ellipsoids are at the 20 % probability level

Table 1 Hydrogen bonds for two molecules of ZM 241385 (**9**) [Å and °]

D–H···A	d(D–H)	d(H···A)	d(D···A)	<(DHA)
N(4)–H(4A)…O(5)	0.82(3)	2.19(3)	2.851(3)	137(2)
O(1′)–H(1′B)…N(7)	0.90(4)	1.81(4)	2.689(2)	165(3)
O(1)–H(1B)…N(7′)	0.96(4)	1.75(4)	2.697(2)	168(3)
N(4′)–H(4′A)…O(3)	0.82(3)	2.49(3)	3.307(3)	175(2)
N(1)–H(1A)…O(4)	0.89(3)	2.21(3)	3.026(3)	153(3)
O(3)–H(3A)…N(6′)	1.00(4)	1.87(4)	2.826(3)	160(3)
O(7)–H(7D)…O(6)	1.094(17)	1.831(19)	2.922(4)	175(5)
N(4)–H(4B)…N(2′)$^{\#1}$	0.82(3)	2.13(3)	2.942(3)	172(3)
N(1′)–H(1′A)…O(5)$^{\#2}$	0.87(3)	2.09(3)	2.927(2)	163(2)
N(4′)–H(4′B)…N(2)$^{\#2}$	0.87(3)	2.20(3)	3.048(3)	163(2)
O(5)–H(5A)…O(1′)$^{\#3}$	0.77(3)	2.04(3)	2.808(3)	175(3)
O(4)–H(4D)…O(3)$^{\#1}$	0.93(4)	1.86(4)	2.776(3)	168(3)
O(4)–H(4C)…O(7)$^{\#4}$	0.88(4)	1.95(4)	2.807(3)	163(3)
O(8)–H(8D)…O(6)$^{\#5}$	1.02(4)	1.82(4)	2.832(4)	173(5)
O(8)–H(8C)…N(3)$^{\#6}$	1.02(4)	2.17(5)	3.158(3)	162(6)

Symmetry transformations used to generate equivalent atoms: $^{\#1}$ x, y + 1, z + 1; $^{\#2}$ x, y−1, z−1; $^{\#3}$ −x + 3, −y + 2, −z + 3; $^{\#4}$ −x + 1, −y + 1, −z + 1; $^{\#5}$ −x + 1, −y, −z; $^{\#6}$ x−1, y−1, z−1

ZM 241385 (**9**) changes dramatically between the two structures (Fig. 11b, c). Consequently, the adenosine receptor has space to accommodate the inherent flexibility of the tyramine moiety.

Herein, we extensively compare the ZM 241385 (**9**) coordinates obtained from the two available crystal

Table 2 Comparison of torsion angles within the triazine portion of the ZM 241385 heterocycle

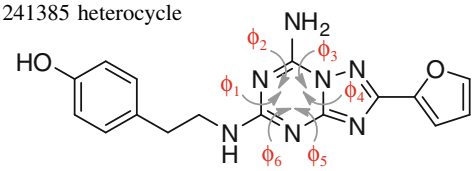

Source	Φ_1	Φ_2	Φ_3	Φ_4	Φ_5	Φ_6
PDB 3EML	1.2°	−0.8°	0.3°	0.0°	0.3°	−0.9°
PDB 3PWH	−0.1°	−0.1°	0.1°	−0.1°	0.1°	−0.1°
ZM 241385 structure 1	−0.7°	6.0°	−5.2°	−1.4°	6.4°	−5.6°
ZM 241385 structure 2	1.8°	−1.3°	0.4°	0.3°	0.1°	−1.2°

structures of the ligand in complex with the adenosine A_{2A} receptor [5, 6] with that of the unbound crystal structure of ZM 241385 (**9**) presented here (two molecules per unit cell).

The overlay of the four ZM 241385 (**9**) structures revealed that the tyramine portion of the ligand can adopt different conformations depending on the structural context (Fig. 11a; Table 3). Most interestingly, the adenosine A_{2A} receptor appears to be able to recognize two strikingly different conformations of this portion of the tyramine moiety; this was previously noted by Doré et al. [6]. The two structures from the unbound crystal structure of ZM 241385 (**9**) adopted slightly different conformations of

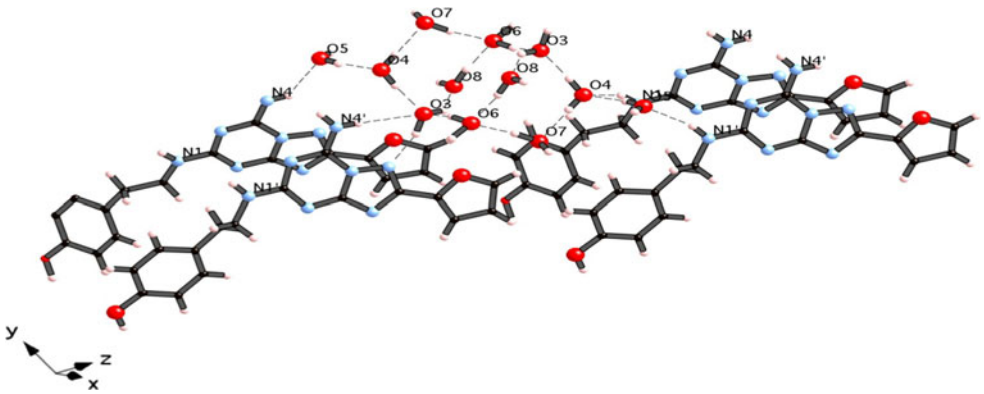

Fig. 10 Partial packing diagram of compound **9**, showing the cluster of water molecules which helps to stabilize the crystal by forming hydrogen bond between layers of the ligand

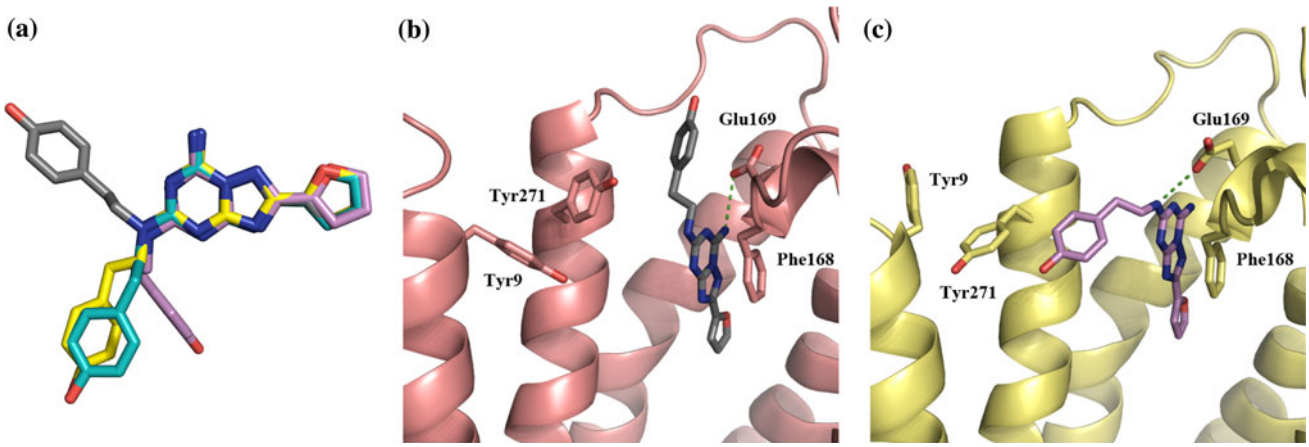

Fig. 11 **a** Overlay of four ZM 241385 structures. *Yellow carbons*—ZM 241385 structure 1; *teal carbons*—ZM 241385 structure 2; *gray carbons*—ZM 241385 in complex with A_{2A} receptor (PDB 3EML); *violet carbons*—ZM 241385 in complex with A_{2A} receptor (PDB 3PWH). **b** ZM 241385 (*gray*) in complex with A_{2A} receptor/lysozyme fusion (*pink*) (PDB 3EML). **c** ZM 241385 (*violet*) in complex with thermostabilized A_{2A} receptor (*yellow*) (PDB 3PWH). Transmembrane helices 2 and 3 removed from figures of complex structures for clarity. *Blue* and *red colors* represent oxygen and nitrogen atoms, respectively (Color figure online)

Table 3 Comparison of torsion angles for the tyramine portion of ZM 241385 (**9**)

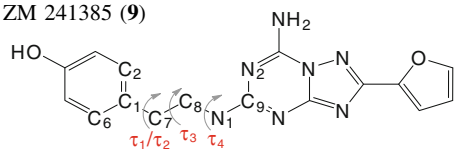

τ_1: C2-C1-C7-C8
τ_2: C6-C1-C7-C8
τ_3: C1-C7-C8-N1
τ_4: C7-C8-N1-C9

Source	τ_1/τ_2	τ_3	τ_4
PDB 3EML	−43.2°/135.7°	−176.1°	91.6°
PDB 3PWH	−165.7°/14.0°	140.4°	107.8°
ZM 241385 structure 1	−70.3°/110.7°	−171.1°	−167.9°
ZM 241385 structure 2	−68.8°/112.7°	159.3°	89.5°

the tyramine portion of the ligand, which resided in between the two extremes of the structures obtained by Doré et al. [6] and Jaakola et al. [5]. As shown in Fig. 11b, c, the conformation of Glu169 also changes between the two crystal structures, resulting in hydrogen bonds in different locations of ZM 241385. Phe168 engages in π-stacking with the triazolotriazine heterocycle in both cases.

Vacuum and explicit aqueous solution conformational searches

Variations in the conformations of the bound ZM 241385 (**9**) and their comparison to the conformations of the unbound compound point to its extensive flexibility. In order to further address this issue, we have extended the structural analysis of ZM 241385 (**9**) and carried out conformational searches for this compound *in vacuo* and in explicit aqueous solution.

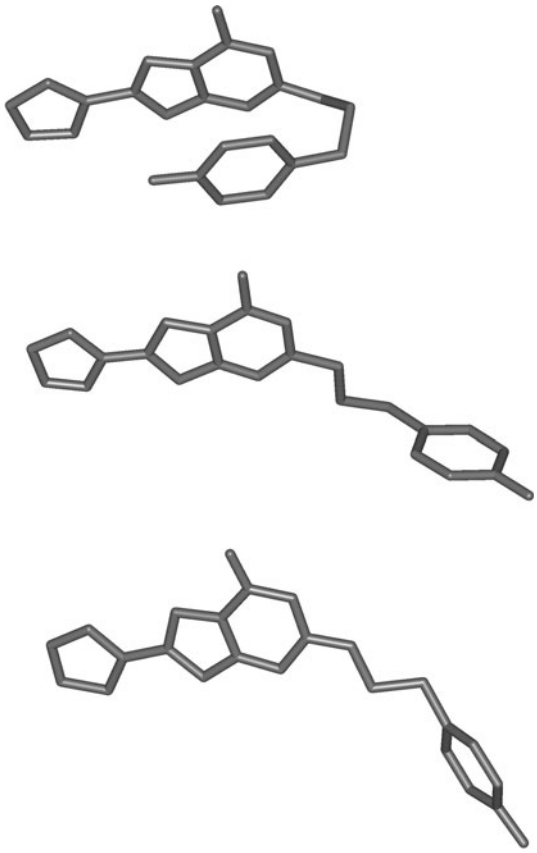

Fig. 12 Conformations of ZM 241385 in different environments. *Top* vacuum (modeled); *middle* explicit aqueous solution (modeled); *bottom* solid state (experimental)

Compound ZM 241385 (**9**) contains a flexible linker, connecting two rigid moieties; a substituted benzene ring and a heterocyclic triazolotriazine ring system. The furan and triazolotriazine rings, the linker itself, as well as the

hydroxyl substituent on the aromatic ring make this molecule fairly hydrophilic. Thus, due to these properties and to the flexibility of the linker, the two ring systems have the ability to interact via intramolecular van der Waals (vdW) and hydrogen bonding interactions, thus potentiating a range of accessible conformations, depending on the environment (Fig. 12).

The lowest energy structure obtained from the conformational search of ZM 241385 (**9**) *in vacuo* featured the phenol portion of the ligand stacking with the heterocycle (Fig. 12 [top]). In solution, two main forces determine the preferred conformation. On one hand, intramolecular vdW and hydrogen bonding interactions favor formation of folded conformations, so as to minimize contact with water for the hydrophobic parts of the molecule (e.g., aromatic ring). On the other hand, the polarizable groups (e.g., hydroxyl) "push" the molecule into bulk solvent, thus aiding the extended form of the compound. While both conformations have been observed in the conformational search carried out in an explicit aqueous environment, the lowest energy conformation was found in the extended state (Fig. 12 [middle]). This conformation is very similar to that in the solid state, except for the torsion angles in the highly flexible linker. The extended conformation of the solid state (Fig. 12 [bottom]) is likely to be a result of the intermolecular interactions in the crystal lattice (discussed above). We have previously observed similar environment-dependent conformational behavior for other molecules containing rigid hydrophobic elements decorated with polarizable groups, and connected by flexible linkers [16–18].

Conclusion

ZM 241385 (**9**) has been successfully synthesized in an overall yield of 5 %. A complete characterization of ZM 241385 (**9**) and its intermediates (**3–6**) has been performed that exhibited some interesting NMR spectral characteristics that have not been reported to date, namely, the doubling up of proton and carbon resonances. Our experiments indicate that these effects are due to the intermolecular interactions, such as dimer formation in combination with hindered rotation. The first single molecule X-ray structure presented in this article confirmed the synthesis of ZM 241385 (**9**) and provided the basis for the structural comparison with the published protein-bound X-ray structure. The overlay of the ZM 241385 (**9**) coordinates revealed that the tyramine portion of the molecule can easily adopt different conformations due to its inherent flexibility. Conformational analyses in vacuum and in explicit aqueous solution allowed an insight into the effect of environment on the conformation.

Experimental

General information

All reactions were stirred magnetically in oven-dried glassware. Anhydrous solvents were transferred via oven-dried syringe or cannula. Technical grade solvents used for extraction and column chromatography were distilled before use. Absolute solvents were used without further purification. Starting materials and reagents **1, 2, 5**, **8** and *m*-CPBA were purchased from Aldrich or AK Scientific in the highest available grade and used without further purification. Compound **10** was purchased from Chembridge Support. Compounds **3**, **4**, **6**, **7**, **9,** and **11** were synthesized in our laboratories. Analytical thin layer chromatography (TLC) plates from Merck were used for reaction control (silica gel 60 on aluminum sheets). Silica gel 60 (Fluka) was used for silica gel flash chromatography. Microwave reactions were performed using a Biotage Initiator 2.0. Proton nuclear magnetic resonance (^{1}H NMR) spectra and carbon-13 nuclear magnetic resonance (^{13}C NMR) spectra were recorded on Bruker spectrometers Avance 400 (400 MHz for ^{1}H and 101 MHz for ^{13}C) at ambient temperature (if not stated differently) in the solvents indicated and referenced to tetramethylsilane (TMS). Spectra measured at 353 K were referenced to d_6-dimethyl sulfoxide (DMSO). Chemical shifts (δ) are reported in parts per million (ppm). Coupling constants (J) are reported in Hertz (Hz). The following abbreviations are used: s (singlet), br s (broad singlet), d, (doublet), t (triplet), q (quartet), and m (multiplet). ^{13}C NMR spectra were routinely run with broadband decoupling. Low resolution electrospray mass spectra (LRMS) using electrospray ionization (ESI) were obtained on a Micromass Platform II spectrometer. Unless otherwise stated, cone voltage was 20 eV. High resolution mass spectra (HRMS) were obtained on a Waters LCT Premier XE (TOF) spectrometer fitted with an electrospray ion source. Mass signals are given in mass units per charge (m/z). The fragments and intensities are written in brackets. Liquid chromatography mass spectra (LCMS) were measured on an Agilent 6100 Series Single Quad LC/MS, Agilent 1200 Series HPLC. (Pump: 1200 Series G1311A Quaternary pump, Autosampler: 1200 Series G1329A Thermostatted Autosampler, Detector: 1200 Series G1314B Variable Wavelength Detector). Gradient takes 4 min to get to 100 % ACN; maintain for 3 min and a further 3 min to get back to the original 5 % ACN. Melting points were measured with a MP50 Melting Point System from Mettler Toledo.

X-ray structure

Intensity data for compound **9** was collected on an Oxford Diffraction SuperNova CCD diffractometer using Cu Kα

radiation. The temperature during data collection was maintained at 130.0(1) K using an Oxford Cryostream cooling device. The structure was solved by direct methods and difference Fourier synthesis [19]. Thermal ellipsoid plot was generated using the program ORTEP-3 [20], integrated within the WINGX [21] suite of programs.

Crystal data for compound **9**. $(C_{16}H_{15}N_7O_2)0{\cdot}3(H_2O)$, $M = 391.40$, $T = 130.0$ K, $\lambda = 1.54180$, triclinic, space group P-1, $a = 10.851(2)$, $b = 13.349(3)$, $c = 15.215(3)$ Å, $\alpha = 107.694(19)°$, $\beta = 101.122(15)°$, $\gamma = 108.736(18)°$. V 1882.4(6) $Å^3$, $Z = 4$, $D_c = 1.381$ Mg M^{-3}, μ(Cu Kα) 0.889 mm^{-1}, $F(000) = 824$ crystal size $0.36 \times 0.32 \times 0.04$ mm^3, 12,553 reflections measured, 6,770 independent reflections [R(int) = 0.0353], the final R was 0.0539 [$I > 2\sigma(I)$] and $wR(F^2)$ was 0.1594 (all data).

Overlay of X-ray structures

The four X-ray structures were overlaid in Maestro 9.2, using only the heterocyclic portion for the superposition. Torsion angles were measured using Maestro 9.2.

Conformational search of ZM 241385 *in vacuo*

Conformational search was carried out using Macromodel 9.9 *in vacuo*. The OPLS_2005 force field was used to parameterize the structure. The Polak–Ribiere conjugate gradient method was used to minimize prospective structures. A maximum of 1,000 iterations with a convergence threshold of 0.1 kcal/mol Å was used for each minimization. The Torsional Sampling method was used to perform the conformational search. Automatic Setup was initially used to identify the search variables, which were subsequently edited. Specifically, torsions within the heterocyclic and furan rings that were automatically selected by Automatic Setup were removed from the search, and all defined ring closures and torsion check parameters were removed. Extended torsion sampling was used, and mirror image conformations were not retained. A maximum of 14,000 conformational search steps were set, corresponding to 2,000 steps per rotatable bond. No limit was specified on the number of structures saved by the search. An energy window of 6 kcal/mol (25.1 kJ/mol) was specified for saving structures.

Explicit solvent conformational search of ZM 241385

An explicit solvent conformational search of ZM 241385 was performed using HyperChem 7.52, following a previously established procedure [17].

Synthesis

*N″-(Furan-2-ylcarbonyl)carbonohydrazonic diamide (**3**)*

Furoic acid hydrazide (**1**) (6.00 g, 47.5 mmol) and *S*-methylisothiosulfate hemisulfate (**2**) (33.1 g, 238 mmol) were added to a solution of sodium hydroxide (3.04 g, 76.1 mmol) in water (150 mL). The clear solution was stirred at room temperature for 24 h and the resultant precipitate was filtered and washed with water and diethyl ether and afterward dried under vacuum. Product **3** (4.60 g, 58 %) was obtained as a white solid, mp: 181–184 °C ([9] 213 °C). ^{1}H NMR (400 MHz, D_2O) δ 7.50 (m, 1H, C*H*–O), 6.87 (m, 1H, C*H*=C), 6.48 (m, 1H, CH=C*H*–CH). ^{13}C NMR (101 MHz, D_2O) δ 158.5 (C), 155.8 (C), 148.4 (C), 144.4 (CH), 112.4 (CH), 111.5 (CH). LRMS: *m/z* (ESI 20 V) 169.2 (MH^+, 100).

*5-(Furan-2-yl)-1H-1,2,4-triazol-3-amine (**4**)*

Method (A) *N″*-(Furan-2-ylcarbonyl)carbonohydrazonic diamide (**3**) (1.00 g, 5.95 mmol) was suspended in water (20 mL). The reaction mixture was stirred in the microwave at 140 °C for 1 h (pressure 6 bar) then cooled to room temperature and the solvent was removed under vacuum. The product **4** was obtained as a beige solid (880 mg, 99 %). ^{1}H NMR (400 MHz, d_6-DMSO) δ 12.02 (s, br, 1H, N*H*), 7.69 (dd, $J = 1.7$, 0.7 Hz, 1H, C*H*–O), 6.69 (d, $J = 3.2$ Hz, 1H, C*H*=C), 6.54 (dd, $J = 3.3$, 1.8 Hz, 1H, CH=C*H*–CH), 6.01 (br s, 2H, NH_2). ^{13}C NMR (101 MHz, d_6-DMSO) δ 157.6 (C), 151.7 (C), 147.3 (C), 142.7 (CH), 111.3 (CH), 107.7 (CH). LRMS: *m/z* (ESI 20 V) 151.2 (MH^+, 100).

Method (B) *N″*-(Furan-2-ylcarbonyl)carbonohydrazonic diamide (**3**) (4.16 g, 24.7 mmol) was suspended in water (85 mL). The reaction mixture was stirred under conventional heating at reflux for 29 h then cooled to room temperature and the solvent was removed under vacuum. The residue was suspended in water (20 mL) and filtered. The filter cake was washed with water and dried under high vacuum. The product **4** (2.96 g, 80 %) was obtained as a pinkish white solid, mp: 198–204 °C ([9] 230 °C). ^{1}H and ^{13}C NMR and mass spectral data are in accordance with above characterization.

*2-(Furan-2-yl)-5-(methylthio)-[1,2,4]triazolo[1,5-a][1,3,5]triazin-7-amine (**6**)*

5-(Furan-2-yl)-1*H*-1,2,4-triazol-3-amine (**4**) (50.0 mg, 333 μmol) and *N*-cyanodithioiminocarbonate (**5**) (48.7 mg, 333 μmol) were mixed and heated at 170 °C for 1 h under a nitrogen atmosphere. The reaction mixture was cooled to room temperature, absorbed on Celite and purified by

column chromatography (dichloromethane: ethyl acetate 95:5 → 85:15). The product **6** (27.0 mg, 32 %) was obtained as a white solid, mp: 237–240 °C ([4, 11] 238–240 °C). ^{1}H NMR (400 MHz, d_6-DMSO) δ 8.97 (br s, 1H, N*H*), 8.78 (br s, 1H, N*H*), 7.94 (dd, J = 1.8, 0.8 Hz, 1H, O–C*H*), 7.17 (dd, J = 3.4, 0.8 Hz, 1H, C–C*H*), 6.72 (dd, J = 3.4, 1.8 Hz, 1H, CH = C*H*–CH), 2.52 (s, 3H, S–CH_3). ^{13}C NMR (101 MHz, d_6-DMSO) 173.3 (C), 157.2 (C), 156.2 (C), 149.6 (C), 145.5 (C), 145.2 (CH), 112.5 (CH), 112.1 (CH), 13.6 (CH_3). LCMS: *m/z* (ESI 20 V) 249.1 (MH^+, 100).

*2-(Furan-2-yl)-5-(methylsulfonyl)-[1,2,4]triazolo[1,5-a][1,3,5]triazin-7-amine (**7**) [4]*

A solution of *meta*-chloroperoxybenzoic acid (1.06 g, 4.48 mmol) in dichloromethane (10 mL) was added dropwise at −5 °C to a suspension of 2-(furan-2-yl)-5-(methylthio)-[1,2,4]triazolo[1,5-*a*][1,3,5]triazin-7-amine (**6**) (278 mg, 1.12 mmol) in dichloromethane (17 mL). The reaction was stirred at room temperature for 22 h before the solvent was removed under vacuum. The crude material was suspended in ethanol (5 mL) and stirred at room temperature for 30 min. The solid was collected by filtration, washed with ethanol and dried to give the title compound **7** (230 mg, 82 %) as a yellowish-white solid, mp: 168 °C (dec). ^{1}H NMR (400 MHz, d_6-DMSO) δ 9.81 (s, 1H, N*H*), 9.48 (s, 1H, N*H*), 7.99 (dd, J = 1.7, 0.8 Hz, 1H, O–C*H*), 7.27 (dd, J = 3.4, 0.7 Hz, 1H, C–C*H*), 6.76 (dd, J = 3.4, 1.8 Hz, 1H, CH = C*H*–CH), 3.37 (s, 3H, S–CH_3). ^{13}C NMR (101 MHz, d_6-DMSO) 165.3 (C), 157.3 (C), 156.8 (C), 152.2 (C), 145.8 (CH), 145.0 (C), 113.4 (CH), 112.3 (CH), 38.9 (CH_3). LCMS: *m/z* (ESI 20 V) 281.0 (MH^+, 100).

*4-(2-((7-Amino-2-(furan-2-yl)-[1,2,4]triazolo[1,5-a][1,3,5]triazin-5-yl)amino)ethyl)phenol (**9**) (ZM 241385)*

Tyramine (**8**) (490 mg, 3.75 mmol) was added to a suspension of 2-(furan-2-yl)-5-(methylsulfonyl)-[1,2,4]triazolo[1,5-*a*][1,3,5]triazin-7-amine (**7**) (250 mg, 892 µmol) in acetonitrile (25 mL). The reaction mixture was stirred overnight at room temperature. After 22 h the solvent was evaporated, the residue was adsorbed on Celite and purified by column chromatography (dichloromethane: methanol 25:75). The collected fractions with product were evaporated to dryness and recrystallized from ethyl acetate. The title compound **9** (100 mg, 33 %) was obtained as a white solid, mp: 229–231 °C ([4] 225–227 °C). ^{1}H NMR (400 MHz, d_6-DMSO, 353 K) δ 8.91 (s, 1H, O*H*), 7.92 (br s, 2H, NH_2), 7.79 (m, 1H, H_{Furan}), 7.14 (br t, 1H, N*H*), 7.04 (m, 3H, 2 × H_{Ar}, H_{Furan}), 6.71 (m, 2H, 2 × H_{Ar}), 6.64 (dd, J = 3.3, 1.8 Hz, 1H, H_{Furan}), 3.49 (m, 2H, CH_2−CH_2−NH), 2.78 (m, 2H, CH_2–CH_2–NH). ^{13}C NMR (101 MHz, d_6-DMSO) δ 161.1 (C), 159.0 (C), 155.9 (C), 155.4 (C), 150.1 (C), 146.1 (C), 144.1 (CH), 129.1 (CH), 115.0 (CH), 111.4 (CH), 111.2 (CH), 42.4 (CH_2), 33.9 (CH_2). HRMS ($C_{16}H_{15}N_7O_2$): Calcd. 338.1360 $[M + H]^+$, Found 338.1353. HPLC: t_R 7.34 min, 98 % (214 nm), 97 % (254 nm).

*[1,2,4]Triazolo[1,5-a][1,3,5]triazin-7-amine (**10**)*

^{1}H NMR (400 MHz, d_6-DMSO) δ 8.95 (br s, 2H, NH_2), 8.53 (s, 1H, C*H*–N–C–NH_2), 8.35 (s, 1H, C*H*). ^{13}C NMR (101 MHz, d_6-DMSO) δ 159.0 (CH), 156.8 (C), 154.7 (CH), 151.8 (C). LCMS: *m/z* (ESI 20 V) 137.2 (MH^+, 100).

*2-(Furan-2-yl)-5-phenethoxy-[1,2,4]triazolo[1,5-a][1,3,5]triazin-7-amine (**11**) [4]*

^{1}H NMR (400 MHz, d_6-DMSO) δ 8.95–8.60 (2 × br s, ratio 1:1, 2H, NH_2), 7.91 (m, 1H, H_{Furan}), 7.32 (m, 4H, H_{Ar}), 7.24 (m, 1H, H_{Ar}), 7.14 (dd, J = 3.4, 0.5 Hz, 1H, H_{Furan}), 6.71 (dd, J = 3.4, 1.8 Hz, 1H, H_{Furan}), 4.52 (t, J = 6.8 Hz, 2H, CH_2–O), 3.05 (t, J = 6.8 Hz, 2H, C$H_2$$CH_2$–O). ^{13}C NMR (101 MHz, d_6-DMSO) δ 164.9 (C), 158.9 (C), 156.6 (C), 151.6 (C), 145.6 (C), 145.1 (CH), 138.1 (C), 128.9 (CH), 128.3 (CH), 126.3 (CH), 112.3 (CH), 112.0 (CH), 67.9 (CH_2), 34.4 (CH_2). HRMS ($C_{16}H_{14}N_6O_2$): Calcd. 323.1251 $[M + H]^+$, found 323.1521. mp: 201–204 °C. HPLC: t_R 9.14 min, >99.5 % (214 nm), >99.5 % (254 nm).

Accessory publication

Crystallographic data (excluding structure factors) for the structure reported in this article has been deposited with the Cambridge Crystallographic Data Centre CCDC 901689. Copies of the data can be obtained free of charge on application to the CCDC, 12 Union Road, Cambridge CB2 1EZ, UK (Fax: +44 1223/336033; deposit@ccdc.cam.ac.uk).

^{1}H and ^{13}C NMR spectra for all synthesized compounds, including HPLC, HRMS, and X-ray structure details of ZM 241385 (**9**) are documented in the supplementary information.

Acknowledgments M.J. is a recipient of the Australian Postgraduate Award Industry (APAI). We thank GlaxoSmithKline, GSK R&D China, Singapore for financial support and Dr. Jason Dang (Monash University) for assistance in obtaining NMR and HRMS data. We also thank Associate Professor Martin Scanlon, Dr Jamie Simpson and Dr James Swarbrick from Monash University for insightful discussions on the NMR aspects in this paper.

References

1. Baraldi PG, Cacciari B, Spalluto G, Borioni A, Viziano M, Dioniotti S, Ongini E (1995) Curr Med Chem 2:707

2. Müller CE (2000) Drug Future 25:1043
3. Richardson PJ, Kase H, Jenner PG (1997) Trends Pharmacol Sci 18(9):338
4. Caulkett PWR, Jones G, Collis MG, Poucher SM (1991). European Patent EP 459702, 23 May 1991
5. Jaakola V-P, Griffith MT, Hanson MA, Cherezov V, Chien EYT, Lane JR, IJzerman AP, Stevens RC (2008) Science 322(5905):1211
6. Doré AS, Robertson N, Errey JC, Ng I, Hollenstein K, Tehan B, Hurrell E, Bennett K, Congreve M, Magnani F, Tate CG, Weir M, Marshall FH (2011) Structure 19(9):1283
7. Minetti P, Tinti MO, Carminati P, Castorina M, Di Cesare MA, Di Serio S, Gallo G, Ghirardi O, Giorgi F, Giorgi L, Piersanti G, Bartoccini F, Tarzia G (2005) J Med Chem 48(22):6887
8. Federico S, Paoletta S, Cheong SL, Pastorin G, Cacciari B, Stragliotto S, Klotz KN, Siegel J, Gao Z-G, Jacobson KA, Moro S, Spalluto G (2011) J Med Chem 54(3):877
9. Srivastava RP, Kumar VV, Bhatia S, Sharma S (1995) Indian J Chem 34B:209
10. Dolzhenko AV, Pastorin G, Dolzhenko AV, Chui WK (2009) Tetrahedron Lett 50:2124
11. Caulkett PWR, Jones G, McPartlin M, Renshaw ND, Stewart SK, Wright B (1995) J Chem Soc Perkin Trans 1:801
12. Kessler H (1970) Angew Chem Int Ed 9:219
13. Lunazzi L, Macciantelli D, Grossi L (1983) Tetrahedron 39(2): 305
14. Anderson JE, Griffith DL, Roberts JD (1969) J Am Chem Soc 91:6371
15. Zhukov A, Andrews SP, Errey JC, Robertson N, Tehan B, Mason JS, Marshall FH, Weir M, Congreve M (2011) J Med Chem 54(13):4312
16. Yuriev E, Kong DCM, Iskander MN (2004) Eur J Med Chem 39(10):835
17. Capuano B, Crosby IT, Forsyth CM, McRobb FM, Moudretski VV, Taylor DA, Vom A, Yuriev E (2010) Struct Chem 21(3):613
18. Golzarroshan B, Siddegowda MS, Li HQ, Yathirajan HS, Narayana B, Rathore RS (2012) J Mol Struct 1018:107
19. Sheldrick G (2008) Acta Crystallogr A 64(1):112
20. Farrugia LJ (1997) J Appl Crystallogr 30(5–1):565
21. Farrugia LJ (1999) J Appl Crystallogr 32(4):837